active site cleft in a manner consistent with previous difference Fourier studies using dinucleotides (*7, 10*). The conformation of the polynucleotide chain is smooth, extended, and exhibits no unacceptable turns or bends.

Finally, we would like to call attention to the fact that the 5′ terminus of the polynucleotide strand is firmly bound on the side of the protein opposite the active site, which is nearly 30 Å away from the catalytic center. It is here, as Matthew and Richards showed (*14*), that there is a cluster of lysine and arginine residues precisely where the 5′ terminal phosphate is found. This cluster of Lys^{31}, Lys^{37}, Lys^{91}, and Arg^{33} forms a strong local positive charge distribution that they predicted would serve as a strong anion binding site.

Figure 5 is the RNase molecule with the single DNA strand shown in red, but with lysine amino groups and guanidinium groups of arginines highlighted in yellow along with His^{12} and His^{119}. Apparent in this figure is the linear array of positively charged groups displayed by the protein on its surface and the complementarity between this linear array and the course of the polynucleotide chain. Indeed, we believe that a major consequence of the folding of the polypeptide chain is the presentation of a linear sequence of positive charges in three-dimensional space that traces the path of a polynucleotide chain and serves to lead it through the active site of the enzyme without distortion and in a manner consistent with its chemical and conformational preferences.

REFERENCES AND NOTES

1. C. B. Anfinsen and F. H. White, Jr., in *The Enzymes*, P. D. Boyer, Ed. (Academic Press, New York, ed. 2, 1961), vol. 5.
2. F. M. Richards and H. Wyckoff, in *The Enzymes*, P. D. Boyer, Ed. (Academic Press, New York, ed. 3, 1971), vol. 4.
3. P. Blackburn and S. Moore, in *The Enzymes*, P. D. Boyer, Ed. (Academic Press, New York, ed. 3, 1982), vol. 15.
4. G. Felsenfeld, G. Sandeen, P. H. von Hippel, *Proc. Natl. Acad. Sci. U.S.A.* **50**, 644 (1963).
5. P. H. von Hippel, D. E. Jensen, R. C. Kelly, J. D. McGhee, in *Nucleic Acid-Protein Recognition*, H. J. Vogel, Ed. (Academic Press, New York, 1977).
6. A. Wlodawer and L. Sjolin, *Biochemistry* **22**, 2720 (1983).
7. A. Wlodawer, in *Biological Macromolecules and Assemblies*, F. A. Jurnak and A. McPherson, Eds. (Wiley, New York, 1984), vol. 2, pp. 393–440.
8. F. G. Walz, *Biochemistry* **10**, 2156 (1971).
9. H. Sekine, E. Nakano, K. Sakaguchi, *Biochim. Biophys. Acta* **174**, 202 (1969).
10. H. W. Wyckoff, W. Carlson, S. Wodak, in *Nucleic Acid-Protein Recognition*, H. J. Vogel, Ed. (Academic Press, New York, 1977), pp. 569–580.
11. D. E. Jensen and P. H. von Hippel, *J. Biol. Chem.* **251**, 7198 (1976).
12. M. T. Record, T. M. Lohman, P. de Haseth, *J. Mol. Biol.* **107**, 145 (1976).
13. R. L. Karpel, V. A. Yrttimaa, G. L. Patel, *Biochem. Biophys. Res. Commun.* **100**, 760 (1981).
14. J. B. Matthew and F. M. Richards, *Biochemistry* **21**, 4989 (1982).
15. G. D. Brayer and A. McPherson, *J. Biol. Chem.* **257**, 3359 (1981).
16. A. McPherson, G. D. Brayer, R. Morrison, *Biophysical J.* **49**, 109 (1986).
17. A. McPherson *et al.*, *J. Mol. Biol.*, in press.

18. Supported by grant 21398 from NIH (A.M.). G.D.B. was a recipient of a fellowship from the Canadian Medical Research Council. We thank Ms. Marie Greene and Mr. Gregory DeLozier for production of graphics and Ms. Lindsay Robinson for technical assistance.

9 December 1985; accepted 1 April 1986

Identification and Characterization of the Protein Encoded by the Human N-*myc* Oncogene

DENNIS J. SLAMON, THOMAS C. BOONE, ROBERT C. SEEGER, DUANE E. KEITH, VICKI CHAZIN, HYUN C. LEE, LAWRENCE M. SOUZA

The human N-*myc* gene is related to the c-*myc* proto-oncogene, and has been shown to have transforming potential in vitro. Many studies have reported amplification of N-*myc* in human neuroblastoma and retinoblastoma cell lines. In primary tumors, amplification of the gene was found to correlate directly with behavior of the tumor. Specific restriction fragments of a partial complementary DNA clone of N-*myc* from LA-N-5 human neuroblastoma cells were placed into a bacterial expression vector for the purpose of producing antigens representative of the N-*myc* protein. Rabbits immunized with these antigens produced antisera that recognized a protein of 62–64 kilodaltons in neuroblastoma cells. By several criteria, this protein appears to be part of the same proto-oncogene family as the c-*myc* protein. Moreover, the antisera to fragments of this protein were capable of histochemically identifying malignant cells in clinical specimens.

THE N-*MYC* GENE, WHILE NOT A classic proto-oncogene in that it does not have a homolog carried by an acutely transforming retrovirus, is grouped with the proto-oncogenes because of its homology with c-*myc* (*1, 2*). There is clear evidence for the transforming potential of this gene since N-*myc* can substitute for c-*myc* in the co-transformation assay in which secondary rat embryo cells are transformed into tumorigenic cells (*3*). Thus far, the strongest clinical correlation between alteration of a specific proto-oncogene and human neoplasia has been found in studies of the N-*myc* gene in neuroblastomas. This gene was first identified in human neuroblastoma cell lines where homogeneously staining regions (HSR) on chromosomes (*4*) or double minute (DM) chromosomes (*5*) were frequent. In these cell lines there is a 25- to 700-fold amplification of a gene that is related to, but distinct from, the c-*myc* proto-oncogene (*1, 2*). Amplification and/or increased expression of this gene has been found in untreated primary human neuroblastomas (*6*) and retinoblastomas (*7*). Initial studies of primary neuroblastomas demonstrated that amplification of N-*myc* was correlated with stage of disease; amplification was not found in localized tumors (stages I and II), but was present in 50% of advanced tumors (stages III and IV) (*6*). In a larger study, amplification of the gene in primary neuroblastomas was found to correlate strongly with rapid disease progression and poor clinical prognosis, independent of disease stage at diagnosis (*8*). Thus, amplification of the N-*myc* gene appeared to be more prognostic than clinical staging of the disease.

The strong correlation between N-*myc* gene alterations in primary human tumors and clinical behavior, as well as the transforming potential of the gene in vitro, has led to speculation that it may be involved in the pathogenesis of some human malignancies. To further characterize this gene and its gene product, we undertook experiments to clone and express human N-*myc*. By means of the Okayama-Berg vector (*9*), a complementary DNA library was constructed from the LA-N-5 human neuroblastoma cell line. Approximately 80,000 clones were screened with the pNb-1 probe (*1*), and one clone, N-*myc*1, was obtained. The largest open reading frame in the sequence from N-*myc*1

D. J. Slamon and D. E. Keith, Division of Hematology-Oncology, Department of Medicine, and Jonsson Comprehensive Cancer Center, UCLA School of Medicine, Los Angeles, CA 90024.
T. C. Boone, V. Chazin, L. M. Souza, Amgen, Thousand Oaks, CA 91320.
R. C. Seeger and H. C. Lee, Department of Pediatrics, Jonsson Comprehensive Cancer Center, and Childrens Cancer Study Group, UCLA School of Medicine, Los Angeles, CA 90024.

(Fig. 1) is 1182 nucleotides long, and would encode the COOH-terminal 394 amino acids of a putative N-*myc* protein. A complete sequence of the N-*myc* gene was recently published (*10*), and comparison of the large open reading frame from the N-*myc*1 clone and the published sequence shows only one notable difference. The third base of the codon for amino acid 227 is a cytosine and the first base of the next codon is a guanine in the N-*myc*1 clone. The published sequence shows a reversal of these two residues. This difference results in a change in amino acid 227—alanine instead of proline.

To identify and characterize the N-*myc* gene product, we developed antibody reagents based on the large open reading frame in the N-*myc*1 clone. This was done by constructing a series of expression vectors for the purpose of producing portions of the putative N-*myc*–encoded protein in *Escherichia coli*. Constructs were made by fusing, in frame, the 5′ region of a bovine growth hormone gene (bGH) to the six regions of the N-*myc* gene defined by specific restriction endonuclease sites (Fig. 1). The three sites in the bGH gene used for the fusion to N-*myc*–specific sequences were Sst I, Pst I, and Hind III, generating fusion proteins containing 76, 92, and 114 residues of the NH_2-terminus of bGH, respectively. We utilized the expression vector p414/936, a modified temperature-sensitive runaway plasmid containing (i) a selectable drug marker, Amp^R; (ii) a transcription terminator; and (iii) translation termination signals in all three reading frames. These terminators were adjacent to a polylinker used for introduction of genes linked to a tryptophan synthetase promoter. This vector was used for bGH/N-*myc* constructions I, III, IV, V, and VI, while bGH/N-*myc* II was expressed by means of a similar vector (pCFM414) that had been used to express human c-*myb* (*11*). The bGH/N-*myc* fusion proteins I–V were terminated by translation terminators provided by the expression vectors, while VI terminated with the natural COOH terminus of the N-*myc* protein (Fig. 1). These bGH/N-*myc* fusion proteins were then used to generate polyclonal antisera in rabbits, as previously described (*12*).

Analysis of the N-*myc* nucleotide sequence predicts a protein with some similarities to the c-*myc* protein in terms of size, abundance, and location of basic amino acids (*10*). Antisera generated to the N-*myc* protein fragments were tested in a liquid phase immunoprecipitation assay with human neuroblastoma cell lines (LA-N-5 and IMR-32) that are known to express N-*myc* transcripts, but not c-*myc* (Fig. 2A). The human promyelocytic cell line, HL-60, was used as a negative control, since these cells express high levels of c-*myc* transcripts, but not N-*myc* (Fig. 2A). In addition, two other human cell lines, HT29 (colon carcinoma) and U251 (glioma), were used as negative controls, since neither express N-*myc* transcripts (*13*). The criteria used to identify a protein as N-*myc*–encoded were twofold. First, the protein had to be immunoprecipitated from neuroblastoma cell lysates by antisera to at least two different N-*myc*–encoded fragments representing separate areas of the deduced amino acid sequence, thus greatly reducing the possibility that the immunoprecipitation was due to chance sequence homology between the vector-expressed fragment and a cellular protein other than N-*myc*. Second, the protein should not be found in other human tumor cell lines (including the neural-derived glioma cells) where the N-*myc* transcript is not found.

A protein appearing as a doublet of 62 and 64 kilodaltons (kD) was consistently immunoprecipitated from LA-N-5 human neuroblastoma cells (Fig. 2B, lanes 2, 5, 9–12). Similar results were seen for the IMR-32 human neuroblastoma cell line (*13*). Immunoprecipitation of this protein could be completely competed away by addition of the appropriate N-*myc* fragment to the reaction mix in all cases, indicating a specific antigen-antibody reaction. Examples of the competition reaction are shown (Fig. 2, lanes 3 and 6). Moreover, immunoprecipitation of the doublet protein could not be blocked when nonhomologous antibody and antigen combinations were used; attempts to block precipitation mediated by antisera to fragment II with fragment I antigen was unsuccessful, again indicating that the precipitation was due to a specific antigen-antibody reaction (Fig. 2B, lane 7). Finally, to ensure that the precipitation of the doublet protein was due to antibodies directed to the N-*myc* and not the bGH

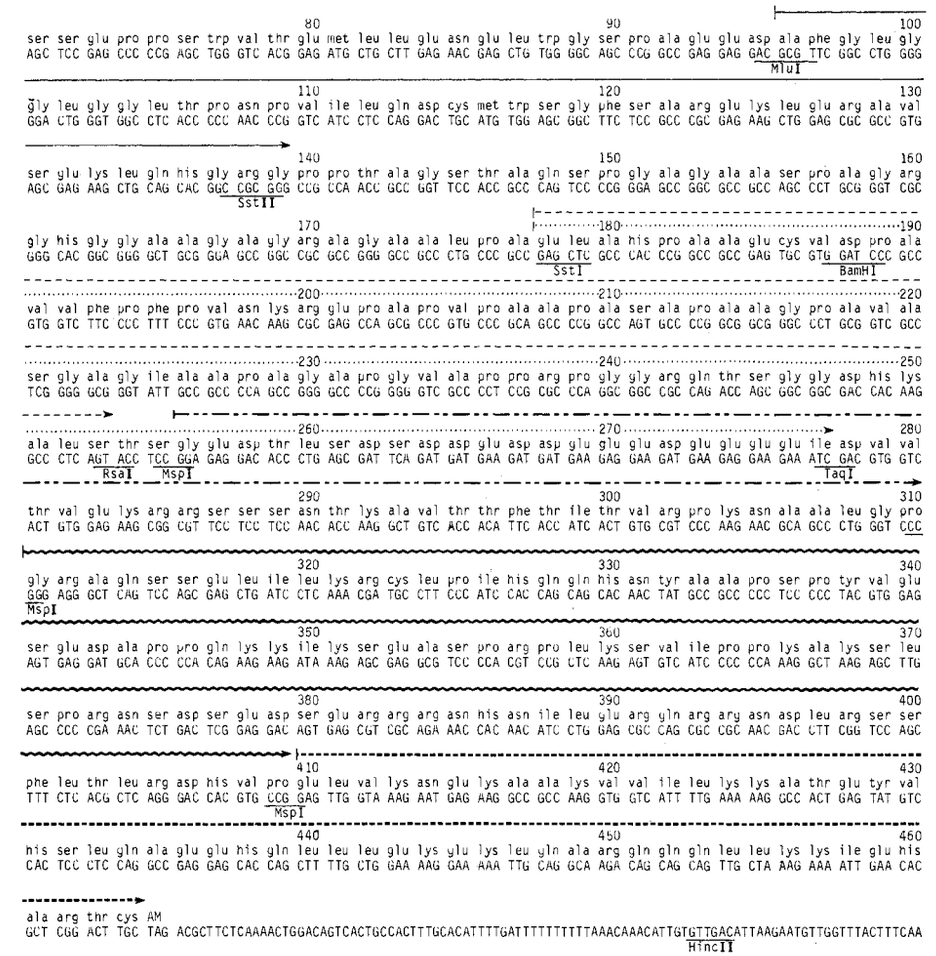

Fig. 1. Nucleotide sequences of the coding region contained in complementary DNA clone N-*myc*1. Dideoxy sequencing was performed on independent M13 clones containing either overlapping fragments or complementary DNA strands. The deduced amino acid sequence is shown immediately above the DNA sequence, and the amino acids are numbered corresponding to the complete sequence (*10*). Specific restriction endonuclease sites used in constructing the bGH/N-*myc* fusion genes are shown underlined and labeled. The N-*myc* portion of each bGH/N-*myc* fusion product is displayed: (——) bGH/*myc* I; (- - -) bGH/N-*myc* II; (·····) bGH/N-*myc* III; (— - - —) bGH/N-*myc* IV; (∿∿) bGH/N-*myc* V; and (- · -) bGH/N-*myc* VI.

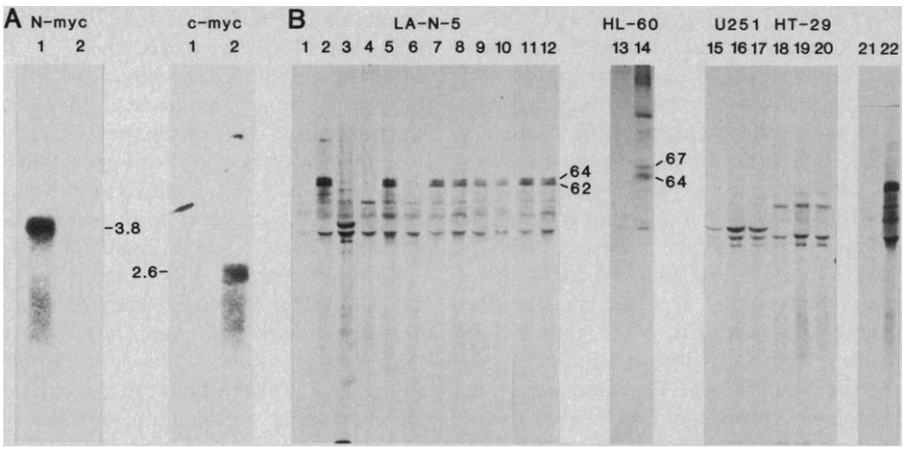

Fig. 2. (A) Northern blot analysis of polyadenylated [poly(A)$^+$] RNA from LA-N-5 human neuroblastoma cells and HL-60 human promyelocytic leukemia cells. Equal amounts (7 μg) of poly(A)$^+$ RNA from LA-N-5 (lane 1) or HL-60 (lane 2) were loaded on 1.1% agarose gel, separated by electrophoresis, transferred to nitrocellulose, and hybridized to either the pNb1 N-*myc* probe (*1*) or a c-*myc*–specific probe, as previously described (*24*). Sizes are shown in kilobases. (B) Immunoprecipitation from various cell lines with antisera directed against the bGH/N-*myc* fragments. Indicated lanes are: (lane 1) LA-N-5 cell lysate and preimmune rabbit sera; (lane 2) LA-N-5 cell lysate and anti–bGH/N-*myc* I; (lane 3) LA-N-5 cell lysate and anti–bGH/N-*myc* I; the antiserum had previously been incubated for 30 minutes at 4°C with 10 μl of solution (1 mg/ml) of the bGH/N-*myc* I fusion protein; (lane 4) LA-N-5 cell lysate and preimmune rabbit serum; (lane 5) LA-N-5 cell lysate and anti–bGH/N-*myc* II; (lane 6) LA-N-5 cell lysate and anti–bGH/N-*myc* II that had been preincubated with the bGH/N-*myc* II fusion protein as above; (lane 7) LA-N-5 cell lysate and antiserum to bGH/N-*myc* II that had been preincubated with bGH/N-*myc* I fusion protein as above; (lane 8) LA-N-5 cell lysate and anti–bGH/N-*myc* II that had been preincubated with bGH alone as above; (lane 9) LA-N-5 cell lysate and anti–bGH/N-*myc* III; (lane 10) LA-N-5 cell lysate and anti–bGH/N-*myc* IV; (lane 11) LA-N-5 cell lysate and anti–bGH/N-*myc* V; (lane 12) LA-N-5 cell lysate and anti–bGH/N-*myc* VI; (lane 13) HL-60 cell lysate and preimmune serum; (lane 14) HL-60 cell lysate and anti–bGH/N-*myc* V; (lanes 15–17) U251 cell lysate and anti–bGH/N-*myc* I, II, and III, respectively; (lanes 18–20) HT-29 cell lysate and anti–bGH/N-*myc* IV–VI, respectively; (lane 21) LA-N-5 cell lysate labeled with ^{32}P-orthophosphate (ICN Biochemicals, Inc., Irvine, CA) and preimmune serum; (lane 22) LA-N-5 cell lysate labeled with ^{32}P-orthophosphate and anti–bGH/N-*myc* II. Total cellular lysates were labeled with [^{35}S]methionine (unless otherwise specified), lysed, reacted with antisera, and analyzed as previously described (*12, 25*). Sizes are shown in kilodaltons.

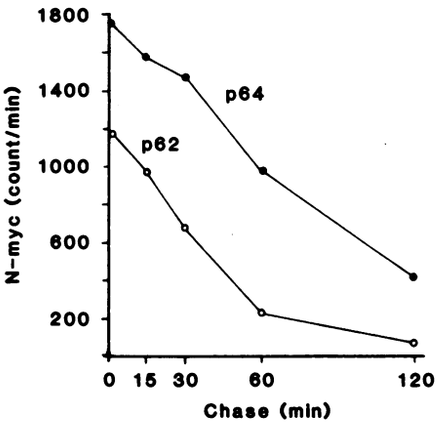

Fig. 3. Kinetics of N-*myc* turnover in LA-N-5 human neuroblastoma cells. Cells were labeled with [^{35}S]methionine for 60 minutes, washed, placed in culture media containing 5×10^4-fold excess of unlabeled methionine, lysed, and analyzed by gel electrophoresis (*12*). The radioactivity associated with the 62–64 kD band at each time point was eluted out of the gel (*12*) and counted.

portion of the fusion protein, bGH alone was added to the reaction mix. In no instance did the bGH compete away the precipitation of the doublet protein. An example of the bGH competition assay is shown in Fig. 2B, lane 8.

The c-*myc* protein is similar in size (64–67 kD) and appearance (doublet) (*14*) to the N-*myc* protein. Like c-*myc* (*14*), the N-*myc* protein is a phosphoprotein (Fig. 2B, lanes 21 and 22). Evidence that this was not the c-*myc* protein, however, is provided by two sets of data. First, the protein identified with the anti-bGH/N-*myc* fusion antibodies was found in cells (LA-N-5) that lack detectable c-*myc* transcripts (Fig. 2A). Secondly, five of the six antisera did not identify any specific protein when used in immunoprecipitation assays with lysate from the HL-60 cell line, which is rich in c-*myc* transcripts (Fig. 2A), indicating that they did not recognize the c-*myc* protein (*13*). The antisera directed against N-*myc* fragment V did recognize a doublet of 64–67 kD in the lysate from HL-60 cells on long exposure (96 hours) of the immunoprecipitation radioautograph (Fig. 2B, lane 14). Comparison of the deduced amino acid sequence from this fragment of N-*myc* and the analogous area in the c-*myc* protein shows significant sequence homology (*10*), which would account for the ability of this antiserum to recognize the c-*myc* protein. None of the antisera to bGH/N-*myc* precipitated a protein of 62–64 kD in the control cell lines U251 and HT-29. Examples of these reactions are shown in Fig. 2B, lanes 15–20. Thus, the data demonstrate that the 62–64 kD protein is the N-*myc*–encoded protein (p62–64$^{N\text{-}myc}$).

The level of N-*myc* protein synthesis in LA-N-5 neuroblastoma cells was estimated with an immunoprecipitation assay. A known amount of [^{35}S]methionine–labeled whole cell lysate was treated with a combination of N-*myc*–specific antisera (anti–bGH/N-*myc* II and IV) and the precipitated proteins were then subjected to sodium dodecyl sulfate–polyacrylamide gel electrophoresis. The p62–64$^{N\text{-}myc}$ was eluted from the gel, and the incorporated [^{35}S] methionine was compared to the total trichloroacetic acid–precipitable incorporation in the lysate (*12*). Approximately 0.016% of the total [^{35}S]- methionine incorporation in these cells was associated with the N-*myc* protein.

The kinetics of intracellular turnover of p62–64$^{N\text{-}myc}$ were determined by pulse-chase labeling experiments. The half-life of the p62–64$^{N\text{-}myc}$ doublet was between 30 and 50 minutes (Fig. 3). Again, this feature of the N-*myc* protein is shared with c-*myc*, which has a half-life of 20 to 30 minutes (*14*). The short half-lives of these two *myc* proteins places them in a group of some of the most rapidly metabolized proteins known (*15*).

To determine the subcellular localization of p62–64$^{N\text{-}myc}$ each of the anti–N-*myc* sera were used in immunocytochemical analyses of LA-N-5 cells. By means of an indirect immunoperoxidase staining procedure and dilutions of N-*myc* antisera of 1:2000 to 1:4000, a strong staining reaction was noted in the nuclei of the cells (Fig. 4A, panel 1). All cells showed nuclear staining; however, the intensity of the stain varied from cell to cell, indicating heterogeneity in N-*myc* protein content. While all six of the anti–N-*myc* antisera recognized p62–64$^{N\text{-}myc}$ in LA-N-5 cells by immunoprecipitation assay, only three of these sera stained the neuroblastoma cells histochemically (anti–N-*myc* II, III, and V). The fact that anti–N-*myc* I, IV, and VI did not react immunocytochemically could be due to fixative-mediated alterations of the antigenic determinants to which the non-reacting antisera are directed. Alternatively, these regions of the protein may be unavailable for recognition by the particular antisera, due to interactions of the antigenic regions with other cellular macromolecules or to the tertiary structure of N-*myc* within intact cells. To determine the

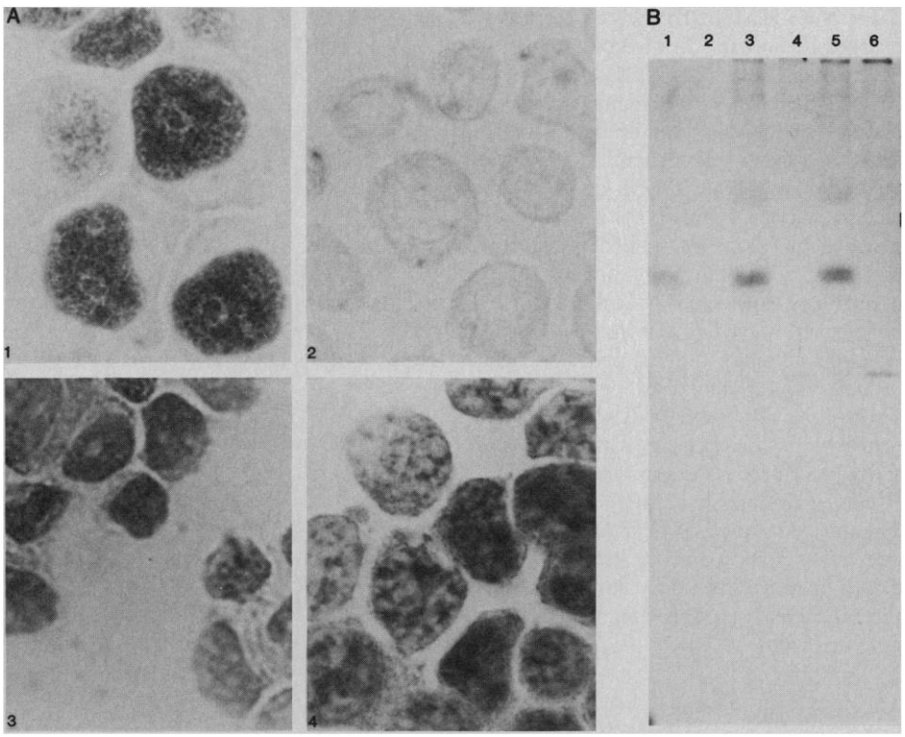

Fig. 4. (A) Immunoperoxidase staining of LA-N-5 human neuroblastoma and HL-60 human promyelocytic leukemia cells with anti-N-*myc* sera. Nuclei of LA-N-5 cells (panel 1) reacted strongly, whereas those of HL-60 cells (panel 2) did not react with anti–bGH/N-*myc* II. In contrast, both LA-N-5 cells (panel 3) and HL-60 cells (panel 4) were reactive with anti–bGH/N-*myc* V. Cultured cells were placed onto coverslips by cytocentrifugation, fixed with 2% paraformaldehyde, treated with phenylhydrazine to block endogenous peroxidase, incubated with antisera (1:3000 dilution) for 18 hours, and then reacted with biotinylated goat anti-rabbit serum followed by reaction with avidin-biotin-peroxidase complexes. Bound peroxidase was visualized with diaminobenzidene/H_2O_2; cells were not counterstained; therefore, all staining was due to reaction between the primary antiserum and *myc* proteins. (B) Subcellular and subnuclear localization of the N-*myc* protein LA-N-5 cells were fractionated (*12*) into nuclear, cytoplasmic, and membrane fractions; each fraction was separately analyzed by immunoprecipitation assay. Indicated lanes are: (lane 1) LA-N-5 cytoplasmic fraction and anti–bGH/N-*myc* II; (lane 2) LA-N-5 membrane fraction and anti–bGH/N-*myc* II; (lane 3) LA-N-5 nuclear fraction and anti–bGH/N-*myc* II. Isolated, intact LA-N-5 nuclei were subfractionated (*16*) into nucleoplasm, chromatin, and nuclear matrix components and analyzed by immunoprecipitation assay: (lane 4) nucleoplasm and anti–bGH/N-*myc* II; (lane 5) nuclear matrix and antiserum to bGH/N-*myc* II; (lane 6) chromatin and anti–bGH/N-*myc* II. The small amount of N-*myc* protein visible in the cytoplasm probably represents de novo synthesis; on the basis of histochemical staining, there was no accumulation in the cytoplasm.

specificity of the cytochemical reaction, HL-60 cells were used as a control. Two of the three antisera (antibGH/N-*myc* II and III) did not stain HL-60 cells, indicating specificity for the N-*myc* protein (Fig. 4A, panels 1 and 2). The antisera directed against N-*myc* fragment V stained both LA-N-5 and HL-60 cells (Fig. 4A, panels 3 and 4). As with the immunoprecipitation data, the ability of this antiserum to immunocytochemically recognize both the N-*myc* and c-*myc* proteins is probably due to the high degree of homology between the two proteins in this region.

The nuclear localization of the $p62\text{–}64^{N\text{-}myc}$ was confirmed by biochemical fractionation of LA-N-5 cells into nuclear, cytoplasmic, and membrane fractions as described (*12*). The majority of the N-*myc* protein was within the nuclei of neuroblastoma cells, which was consistent with data obtained by immunocytochemical analysis (Fig. 4B, lanes 1–3). Intact nuclei were then fractionated into nucleoplasm, chromatin, and nuclear matrix (*16*), and the fractions were separately tested in immunoprecipitation assays with the anti–N-*myc* II (which is N-*myc*–specific). As has been reported for c-*myc* (*17*), the majority of the N-*myc* protein was associated with the nuclear matrix (Fig. 4B, lanes 4–6).

Finally, to evaluate if the N-*myc* antisera had any clinical diagnostic potential, sections of primary human neuroblastoma tumors were tested by immunohistochemical techniques with anti–N-*myc* II (at dilutions of 1:2000 to 1:4000). Tissues from two separate primary tumors were examined; one from a patient with stage II disease, and one with stage IV disease. In both cases, there was intense and specific staining of malignant neuroblasts, with virtually no staining of the adjacent vascular or stromal tissue (Fig. 5). The tumor from the patient with stage II disease (Fig. 5A) was stroma-rich, with nodular areas of undifferentiated cells. This tumor contains one copy of N-*myc* as measured by Southern blot analysis (*8*). The tumor from the patient with stage IV disease (Fig. 5B) consisted of predominantly undifferentiated neuroblasts with surrounding vascular and stromal elements. It has been shown to contain 200 copies of the N-*myc* oncogene (*8*).

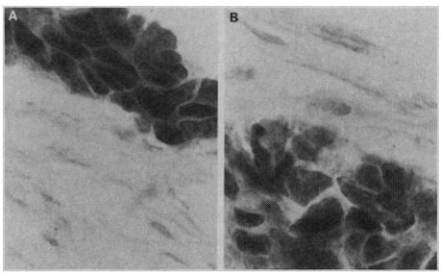

Fig. 5. Immunoperoxidase staining of untreated neuroblastomas with anti–N-*myc* serum. Cryostat sections were prepared and then stained with anti-bGH/N-*myc* II as described in Fig. 4A; all staining visualized is due to reaction of the primary antiserum with N-*myc* protein. (A) Nuclei of undifferentiated neuroblasts stained strongly, whereas the stromal area was nonreactive in the primary tumor from a patient with clinical stage II disease (localized). (B) Nuclei of undifferentiated neuroblasts stained strongly, whereas stroma and blood vessels did not stain in the primary tumor from a patient with clinical stage IV disease (widespread metastases).

The intensity of histochemical staining in these two tumors is equivalent, suggesting similar levels of N-*myc* expression in both specimens (even though one has marked gene amplification). Recent studies with small cell lung carcinoma show high levels of N-*myc* RNA in cells with a single copy of N-*myc* as well as those with amplified N-*myc* (*18*). Taken together, these results indicate that amplification of N-*myc* is only one mechanism by which increased levels of N-*myc* expression are achieved in human tumor cells. Alternative mechanisms may involve changes at the level of control of transcription from single-copy genes.

Our data show that the N-*myc* and c-*myc* proteins are of approximately the same size [62–64 kD (N-*myc*) and 64–67 kD (c-*myc*)], as previously predicted (*10*), are produced as two protein species (doublet) separated by 2–3 kD, are phosphoproteins, are localized to the nucleus of cells, are associated with the nuclear matrix, and have relatively short half-lives. These data indicate that the N-*myc* and c-*myc* proteins constitute separate members of the same proto-oncogene family. This is the second such family to be identified, in that different members of

the *ras* proto-oncogene family also encode similar proteins with respect to size (p21), localization (cytoplasmic membranes), and biochemical properties (binding of guanine nucleotides) (*19*). Functional studies done with the c-*myc* protein have shown it to have a binding affinity for DNA (*17, 20*). It seems likely that N-*myc* also will have an affinity for DNA, based on the numerous basic amino acids found in its COOH terminus. Antibody reagents generated to defined regions of the N-*myc* protein such as those described in this study could prove useful in identifying functional domains.

In addition, antisera to N-*myc* may also have potential clinical utility. The two N-*myc*–specific antisera (II and III) identified for use in histochemical analyses in this study proved to be highly specific for neuroblastoma cells. This could be useful in the sometimes difficult task of differential diagnosis in patients having one of the small round cell tumors of childhood. This group of tumors includes neuroblastomas, neuroepitheliomas, Ewing sarcomas, rhabdomyosarcomas, and lymphomas (*21*). The clinical treatment of these tumors differs greatly; neuroblastomas are not treated in the same manner as lymphomas or Ewing sarcomas. There is evidence that Ewing sarcomas and neuroepitheliomas do not express appreciable levels of N-*myc* (*22*). This is also likely to be true for rhabdomyosarcomas and lymphomas as they are not of neural origin. Thus, a specific histochemically reacting antibody for N-*myc* might be a possible diagnostic reagent. Also, the intensity with which neuroblasts are stained could prove useful in identifying micrometastases in nonprimary sites such as lymph nodes or bone marrow. Finally, correlation of expression of amount of a given proto-oncogene protein with ultimate disease prognosis may be possible with an antibody reagent. Precedent for this already exists with staining for the *ras* gene product in prostatic cancer (*23*).

The identification of the N-*myc* protein and the generation of defined and specific antisera to it should prove helpful in elucidating the role of this gene in human malignancies such as neuroblastoma and small cell lung carcinoma.

REFERENCES AND NOTES

1. M. Schwab *et al.*, *Nature (London)* **305**, 245 (1983).
2. N. E. Kohl *et al.*, *Cell* **35**, 359 (1983).
3. M. Schwab, H. E. Varmus, J. M. Bishop, *Nature (London)* **316**, 160 (1985).
4. J. L. Biedler and B. A. Spengler, *J. Nat. Cancer Inst.* **57**, 683 (1976).
5. J. L. Biedler *et al.*, in *Advances in Neuroblastoma Research*, A. E. Evans, Ed. (Raven, New York, 1980), pp. 81–96.
6. G. M. Brodeur *et al.*, *Science* **224**, 1121 (1984).
7. W. H. Lee, A. L. Murphee, W. F. Benedict, *Nature (London)* **309**, 458 (1984).
8. R. C. Seeger *et al.*, *N. Engl. J. Med.* **313**, 1111 (1985).
9. H. Okayama and P. Berg, *Mol. Cell. Biol.* **2**, 161 (1982).
10. N. E. Kohl *et al.*, *Nature (London)* **319**, 73 (1986).
11. D. J. Slamon *et al.*, *Science*, in press.
12. D. J. Slamon *et al.*, *ibid.* **228**, 1427 (1985).
13. D. J. Slamon, unpublished data.
14. S. R. Hann and R. N. Eisenman, *Mol. Cell. Biol.* **4**, 2486 (1984).
15. A. L. Goldberg and A. C. St. John, *Annu. Rev. Biochem.* **45**, 747 (1976).
16. W. J. Boyle *et al.*, *Mol. Cell. Biol.* **5**, 3017 (1985).
17. R. N. Eisenman *et al.*, *ibid.* p. 114.
18. M. M. Nau *et al.*, *Proc. Natl. Acad. Sci. U.S.A.* **83**, 1092 (1986).
19. J. M. Bishop, *Annu. Rev. Biochem.* **52**, 301 (1983).
20. H. Persson and P. Leder, *Science* **225**, 718 (1984).
21. A. J. Triche and F. B. Askin, in *Pathology of Neoplasia in Children and Adolescents*, M. Feingold, Ed. (Saunders, Philadelphia, in press).
22. M. Israel, personal communication.
23. M. V. Viola *et al.*, *N. Engl. J. Med.* **314**, 133 (1986).
24. D. J. Slamon *et al.*, *Science* **224**, 256 (1984).
25. D. J. Slamon *et al.*, *ibid.* **226**, 61 (1984).

26. Supported by U.S. Public Health Service grant CA 36827 and by National Cancer Institute DHHS grant CA 16042. We thank J. M. Bishop for providing the pNb-1 and pNb-6 N-*myc* clones. We thank L. Ramos, R. Kennedy, and W. Aft for their technical assistance.

18 February 1986; accepted 13 March 1986

Activation of Mouse T-Helper Cells Induces Abundant Preproenkephalin mRNA Synthesis

GERARD ZURAWSKI, MICHAEL BENEDIK,* BARKLEY J. KAMB,† JOHN S. ABRAMS, SANDRA M. ZURAWSKI, FRANK D. LEE

Antigenic or mitogenic stimulation of T cells induces the secretion of an array of protein hormones that regulate immune responses. Molecular cloning has contributed strongly to our present understanding of the nature of this regulation. A complementary DNA (cDNA) library prepared from a cloned concanavalin A–activated mouse T-helper cell line was screened for abundant and induction-specific cDNA's. One such randomly chosen cDNA was found to encode mouse preproenkephalin messenger RNA (mRNA). Preproenkephalin mRNA represented about 0.4 percent of the mRNA in the activated cell line but was absent in resting cells of this line. Other induced T-helper cell lines have 0.1 to 0.5 percent of their mRNA as preproenkephalin mRNA. Induced T-helper cell culture supernatants have [Met]enkephalin-immunoreactive material. The production by activated T cells of a peptide neurotransmitter identifies a signal that can potentially permit T cells to modulate the nervous system.

HELPER T CELLS CAN INDUCE B cells to secrete antibody and can stimulate monocytes, mast cells, and cytotoxic T cells to divide or differentiate. Such T cells, when activated by an antigen or lectin, produce an array of secreted proteins known as lymphokines, which have immunoregulatory activities. Examples of such proteins in the mouse immune system are γ-interferon (γ-IFN), interleukin-2 (IL-2), interleukin-3 (IL-3), and granulocyte-macrophage colony-stimulating factor (GM-CSF) (*1*).

Radiolabeling experiments have shown that, on activation of resting T-helper cells, about 15 percent of newly synthesized proteins appear as secreted products (*2*). In such experiments more secreted protein species are detected than can be accounted for by previously characterized lymphokines. We reasoned that it was important to clone and characterize genes encoding secreted proteins of unknown identity in the hope that they have an as yet undiscovered role in T cell–mediated immune responses. We used a complementary DNA (cDNA) library prepared from the messenger RNA (mRNA) of concanavalin A (Con A)–induced C1.Ly1$^+$2$^-$/9 mouse T-helper cells (*3*). When induced, this cloned T cell line produces secreted activities that regulate the growth and differentiation of lymphoid and myeloid cells (*4*). The cDNA library was probed with ^{32}P-labeled cDNA prepared from oligodeoxythymidine-primed poly(A) mRNA from both resting and induced cells. Approximately 10 percent of the clones hybridized strongly with induced cell probe, but not with resting cell probe. This report describes the characterization of TY3, one such randomly chosen clone.

Clones hybridizing to induction-specific cDNA clone TY3 accounted for about 0.4 percent of the total cDNA's in the library. Hybridization experiments with known lymphokine probes established that TY3 cDNA's do not encode γ-IFN, GM-CSF,

DNAX Research Institute of Molecular & Cellular Biology, 901 California Avenue, Palo Alto, CA 94304.

*Present address: Department of Biology, Texas A & M University, College Station, TX 77843.
†Present address: Department of Biology, Massachusetts Institute of Technology, Cambridge, MA 02139.